AGU ADVANCING EARTH AND SPACE SCIENCES

JGR Space Physics

RESEARCH ARTICLE
10.1029/2026JA035425

Key Points:
- The work shows conjugate hemispheric responses of ionospheric irregularity and convection to magnetopause reconnection
- The magnetic flux tubes opened by dayside reconnection move faster toward the polar cap in the sunlit summer hemisphere
- The hemispheric ionospheric response differences may result from the magnetic reconnection kink degree and the coverage of radar echoes

Correspondence to:
Q.-H. Zhang,
zhangqinghe@nssc.ac.cn

Citation:
Zhang, D., Zhang, Q.-H., Oksavik, K., Lockwood, M., Zhao, J.-C., Zhang, J.-J., et al. (2026). Conjugate ionospheric response to dayside reconnection in both hemispheres. *Journal of Geophysical Research: Space Physics*, *131*, e2026JA035425. https://doi.org/10.1029/2026JA035425

Received 28 MAR 2026
Accepted 12 JUN 2026

Conjugate Ionospheric Response to Dayside Reconnection in Both Hemispheres

Duan Zhang[1], Q.-H. Zhang[1,2], Kjellmar Oksavik[3,4], M. Lockwood[5], Jia-Chen Zhao[2], Jiao-Jiao Zhang[1], Bian-Long Zhao[2], Xiang-Yu Wang[1], Yong Wang[2], Yu-Zhang Ma[2], Zan-Yang Xing[2], Jin Wang[1], and Ling-Xin Zhao[2,6]

[1]State Key Laboratory of Solar Activity and Space Weather, National Space Science Center, Chinese Academy of Sciences, Beijing, China, [2]Shandong Key Laboratory of Space Environment and Exploration Technology, Shandong University, Weihai, China, [3]Department of Physics and Technology, University of Bergen, Bergen, Norway, [4]Arctic Geophysics, University Centre in Svalbard, Longyearbyen, Norway, [5]Department of Meteorology, University of Reading, Reading, UK, [6]School of Integrated Circuits, Shandong University, Jinan, China

Abstract Magnetic reconnection, the dominant process responsible for energy and plasma transport into the magnetosphere, influences plasma circulation in the Earth's polar ionospheres. However, the conjugate response in the two polar ionospheres is not well documented. In this work, based on a case study analysis on 11 February 2004, we used a combination of EISCAT and Super Dual Auroral Radar Network radars in the Northern and Southern Hemispheres to investigate the one-to-one ionospheric response to dayside magnetic reconnection in the two hemispheres under a southward interplanetary magnetic field. A series of flux transfer events generated by magnetic reconnection enhanced the throat convection and voltage in the polar regions. The observations suggest that newly opened magnetic flux tubes in the summer hemisphere moved faster toward the polar cap than in the winter hemisphere due to dayside magnetic reconnection. This hemispheric asymmetry may be due to factors such as magnetic reconnection kink degree, the coverage of radar echoes.

1. Introduction

Magnetic reconnection on the dayside magnetopause is a fundamental plasma process in the solar wind-magnetosphere-ionosphere coupling of high relevance for magnetic storms and substorms (Dungey, 1961; Mozer & Pritchett, 2010). It refers to the process where magnetic field lines with opposite direction components approach each other, generating a thin current sheet. The magnetic field topology changes, and the magnetic field energy is converted into plasma thermal energy, kinetic energy, and high-energy particle acceleration. This is one of the main ways for magnetic field energy to be released in plasmas (Liu et al., 2025; Yamada et al., 2010). When magnetic reconnection occurs due to the interaction between the solar wind and the Earth's magnetic field, the mass, energy and momentum of the solar wind are transferred to the polar ionosphere along nearly vertical magnetic field lines in the polar regions, driving complex dynamic processes such as large-scale convection and particle precipitation (Dungey, 1961; Lyon, 2000; Mende et al., 2016; Zhang et al., 2013). The magnetic reconnection shows an independently intermittent and spatially limited nature (Haerendel et al., 1978), and the associated magnetic signatures are characterized by the transient bipolar variation in the component of the magnetic field normal to the magnetopause (B_N), which are named flux transfer events (FTEs) (Elphic et al., 1990; Haerendel et al., 1978; Russell & Elphic, 1978).

There have been multiple discussions on the ionospheric signatures of FTEs. It is initially signaled by an Alfvénic perturbation propagating from the magnetopause to the ionosphere (Glassmeier & Stellmacher, 1996). Poleward Moving Auroral Forms are the typical ionospheric signatures of the "pulsed" reconnection, usually brightening at the equatorward boundary of the dayside auroral oval and gradually weakening as they enter the polar cap (Drury et al., 2003; Fasel, 1995; Fear et al., 2017; Moen, Oksavik, & Carlson, 2004; Oksavik et al., 2004, 2005; Sandholt & Farrugia, 2007). The ionospheric characteristics include but are not limited to the following: (a) Poleward Moving Radar Auroral Forms (PMRAFs): the poleward-moving regions of backscattering or enhanced back-scattering power (Fear et al., 2017; Milan et al., 2000; Pinnock et al., 1995; Provan et al., 1998); (b) Poleward Moving Plasma Concentration Enhancements (PMPCEs): the poleward-moving regions of high-density plasma, also known as polar cap patches (Carlson et al., 2002, 2004; Zhang et al., 2011); (c) Pulsed Ionospheric Flows or Flow Channel Events: poleward-moving regions of enhanced convection flow in the dayside auroral zone (Moen et al., 2008; Oksavik et al., 2011).

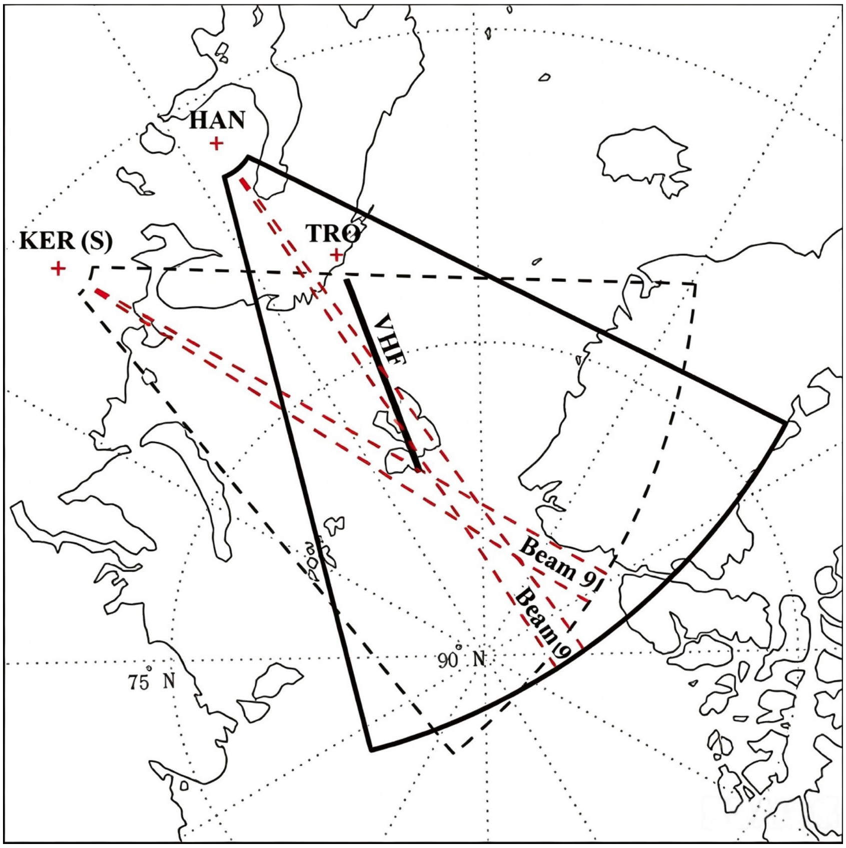

Figure 1. The line-of-sight of the EISCAT Very-High Frequency radar is projected on a geographic map of coastlines (solid black line). The field-of-view of the Hankasalmi radar (HAN) and Kerguelen radar (KER) mapped to the Northern Hemisphere are presented as "fans," together with the specific radar beams used in this study (red dashed lines). Note that KER is in the Southern Hemisphere, so this figure shows its field-of-view mapped to the Northern Hemisphere.

Some studies have shown the conjugate responses of the ionosphere in the Northern and Southern Hemispheres to the magnetospheric dynamical processes and interplanetary magnetic field (IMF) variations (Greenwald et al., 1990; Zou et al., 2023). However, more examples are needed to supplement the differences under different conditions. In this work, based on a case study analysis on 11 February 2004, we compare the poleward-moving events in both hemispheres, including both PMPCEs and PMRAFs, resulting from bursts of magnetopause reconnection, as observed by the EISCAT Very-High Frequency (VHF) radar (Rishbeth & Van Eyken, 1993), and the Hankasalmi (HAN) and Kerguelen (KER) Super Dual Auroral Radar Network (SuperDARN) radar (Chisham et al., 2007; Milan et al., 1997). By using these data sets, this work adopts coordinated dual-hemisphere radar observations to investigate conjugate ionospheric characteristics driven by magnetopause reconnection and analyze their seasonal hemispheric asymmetry including polar convection and cross polar cap potential (CPCP) when the IMF clock angle changes between 180° and 220°, providing new observational evidence for inter-hemispheric ionospheric coupling.

2. Instruments

The EISCAT Scientific Association has a VHF radar near Tromsø (69.58°N, 19.23°E) on the Scandinavian mainland (Folkestad et al., 1983). On 11 February 2004, the EISCAT VHF radar operated at ~224 MHz, with a geographic azimuth of 359.45° and an elevation of 30°, which is indicated by the solid black lines in Figure 1. This radar provides profiles of electron density (Ne), ion and electron temperatures (Ti and Te), and line-of-sight ion velocity (Vi), which help us to detect the plasma characteristics in the polar ionosphere from the sub-auroral latitudes and into the polar cap.

The SuperDARN is composed of more than thirty high-frequency (8–22 MHz) coherent scattering radars distributed in the Northern and Southern Hemispheres for studies of the upper atmosphere and ionosphere (Chisham et al., 2007; Greenwald et al., 1995). The field-of-view of these radars covers a wide area from middle latitudes to polar regions. Under standard operation, a radar typically scans 16 beams, with an interval of 3.24° between adjacent beams. Each beam has a dwell time of 7 s, and a complete scan takes 2 min, covering an azimuth angle of 52° and a range of over 3,000 km. In this study, we use the HAN SuperDARN radar (62.31°N, 26.61°E) in the Northern Hemisphere and the KER SuperDARN radar (49.35°S, 70.27°E) in the Southern Hemisphere, with the field-of-view covering a vast area of the polar regions. Note that the field-of-view mapping of the KER SuperDARN radar to the Northern Hemisphere in Figure 1 is as follows: the radar's geographic field-of-view is first converted to geomagnetic coordinates using Altitude-Adjusted Corrected Geomagnetic coordinates. Then, assuming that the Earth's magnetic field is a dipole field, its conjugate geomagnetic position in the Northern Hemisphere is calculated, which is finally converted back to geographic coordinates. The backscatter power and line-of-sight (l-o-s) Doppler velocity observed by the HAN and KER SuperDARN radars can be used to examine the conjugate ionospheric response to dayside reconnection.

3. Observations and Results

Figures 2a–2c show the (a) Geocentric Solar Magnetospheric IMF Bx/By/Bz components, (b) IMF clock angle ($\theta = \text{atan (By/Bz)}$, $\theta = 0$ along the +z axis), (c) solar wind velocity from Advanced Composition Explorer (ACE) satellite during 11:30 to 13:00 UT on 11 February 2004. ACE orbits the Sun-Earth first Lagrange point (L1), measuring the upstream solar wind and the IMF conditions. A 61-min time delay is applied to the IMF and solar wind data (Liou et al., 1998; Zhang et al., 2011), which roughly matches the period it takes for the IMF and solar wind data obtained by the ACE satellite to propagate to Earth. The calculation of time delay is roughly as follows: (a) the transit time from the ACE satellite to the Earth's bow shock was calculated using this function:

$$t_{\text{transit}} = \frac{X_{\text{SC}}\text{-}X_{\text{BS}}\text{-}\rho \cdot \frac{B_x}{B_\rho}}{V_{\text{SW}}}$$

the meanings of these parameters were described in Liou et al. (1998); (b) The total delay is estimated to be the sum of the t_{transit} + 7 min (+5 min for traversing the magnetosheath and 2 min Alfven transit time) (Lockwood et al., 1989). Figure 2d shows the dayside magnetopause reconnection rate using the parametric function given by Milan et al. (2012). During this period, the IMF Bz component was always negative (southward), while the IMF By component was slightly positive before 11:54 UT and turned negative after this time, favoring a high reconnection rate (Komar & Cassak, 2016). Figures 2e–2h show the (e) electron density, (f and g) electron and ion temperatures, and (h) ion line-of-sight velocity observed by the EISCAT VHF radar during the same period. The open-closed boundary (OCB) in the polar ionosphere, shown by the black dashed lines, corresponds to the high electron temperature edge (Moen, Lockwood, et al., 2004; Zhang et al., 2011). The OCB expanded equatorward due to magnetopause reconnection, and the electron density began to show clear PMPCEs with ion temperature enhancement, as shown by the black lines (marked as "1," "2," etc.). The magenta lines indicate the approximate start time of PMPCEs, and they were almost associated with the enhancement of the dayside magnetopause reconnection rate. It is worth noting that there was a high-density plasma layer around 68° magnetic latitude (MLAT) (100–120 km altitude) after about 12:26 UT, which might be an enhanced or Sporadic E-layer closer to Tromsø. These observations indicate that the OCB carried high-density plasma that was accelerated into the polar cap, consistent with the motion of the newly opened flux tubes resulting from magnetopause reconnection (Carlson et al., 2004; Davis & Lockwood, 1996; Lockwood et al., 2000). For a more detailed analysis, please refer to Zhang et al. (2011).

During the interval of interest, the backscatter power and line-of-sight (l-o-s) Doppler velocity observation results of the HAN SuperDARN radar in the Northern Hemisphere (whose field-of-view covers the observation area of the EISCAT VHF radar) and the KER SuperDARN radar in the Southern Hemisphere (whose field-of-view is roughly conjugate to the HAN radar) are presented in Figures 3a–3d. The field-of-view of the two radars is shown in Figure 1, and the beam used in this work is indicated by the red dashed lines. In Figures 3a and 3b, the PMRAFs observed by the HAN and SuperDARN radars are marked by the black solid lines. These PMRAFs were distributed between 75° and 81° MLAT in the Northern Hemisphere, and between −68° and −76° MLAT in the Southern Hemisphere with a period of about 8–15 min and accompanied by the l-o-s Doppler velocity

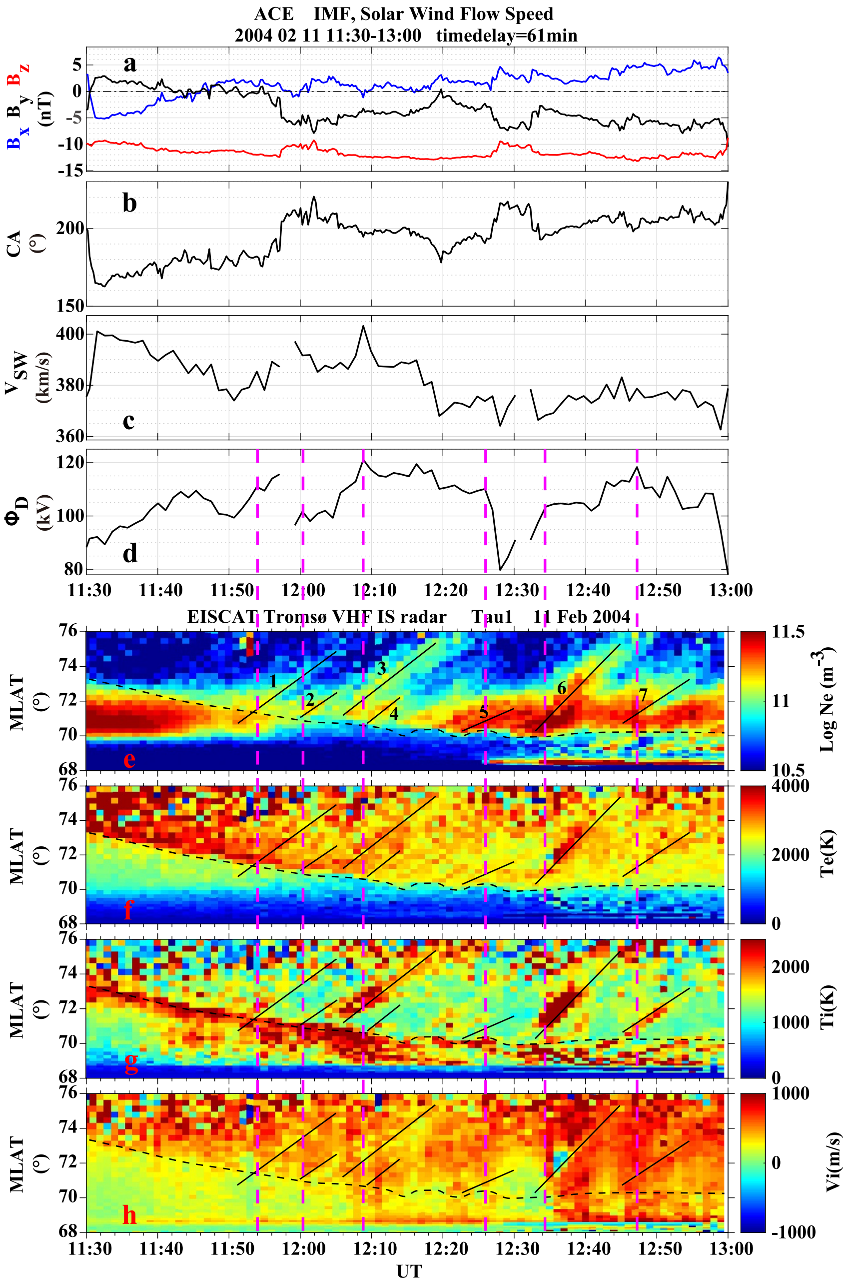

Figure 2. The (a) Geocentric Solar Magnetospheric interplanetary magnetic field (IMF) Bx/By/Bz components, (b) IMF clock angle, (c) solar wind velocity from the Advanced Composition Explorer satellite, and (d) the dayside magnetopause reconnection rate during 11:30 to 13:00 UT on 11 February 2004. A 61-min time delay is applied to the IMF and solar wind data. The (e) electron density, (f and g) electron and ion temperatures, and (h) ion line-of-sight velocity observed by the EISCAT Very-High Frequency radar during the same period. Positive velocities are away from the radar. The black dashed lines highlight the open-closed boundary in the polar ionosphere. The black solid lines highlight the clear Poleward Moving Plasma Concentration Enhancements.

enhancement. The PMRAFs are generally considered as the radar observation features corresponding to the FTEs. These PMRAFs events in the Northern Hemisphere correspond to the poleward-moving events observed by the EISCAT VHF radar, which have been discussed in Zhang et al. (2011). It is interesting that there were no obvious PMRAFs events after 12:35 UT. Moreover, the l-o-s Doppler velocity of the two SuperDARN radars showed that the ionospheric convection was consistently anti-sunward and larger in the Southern Hemisphere.

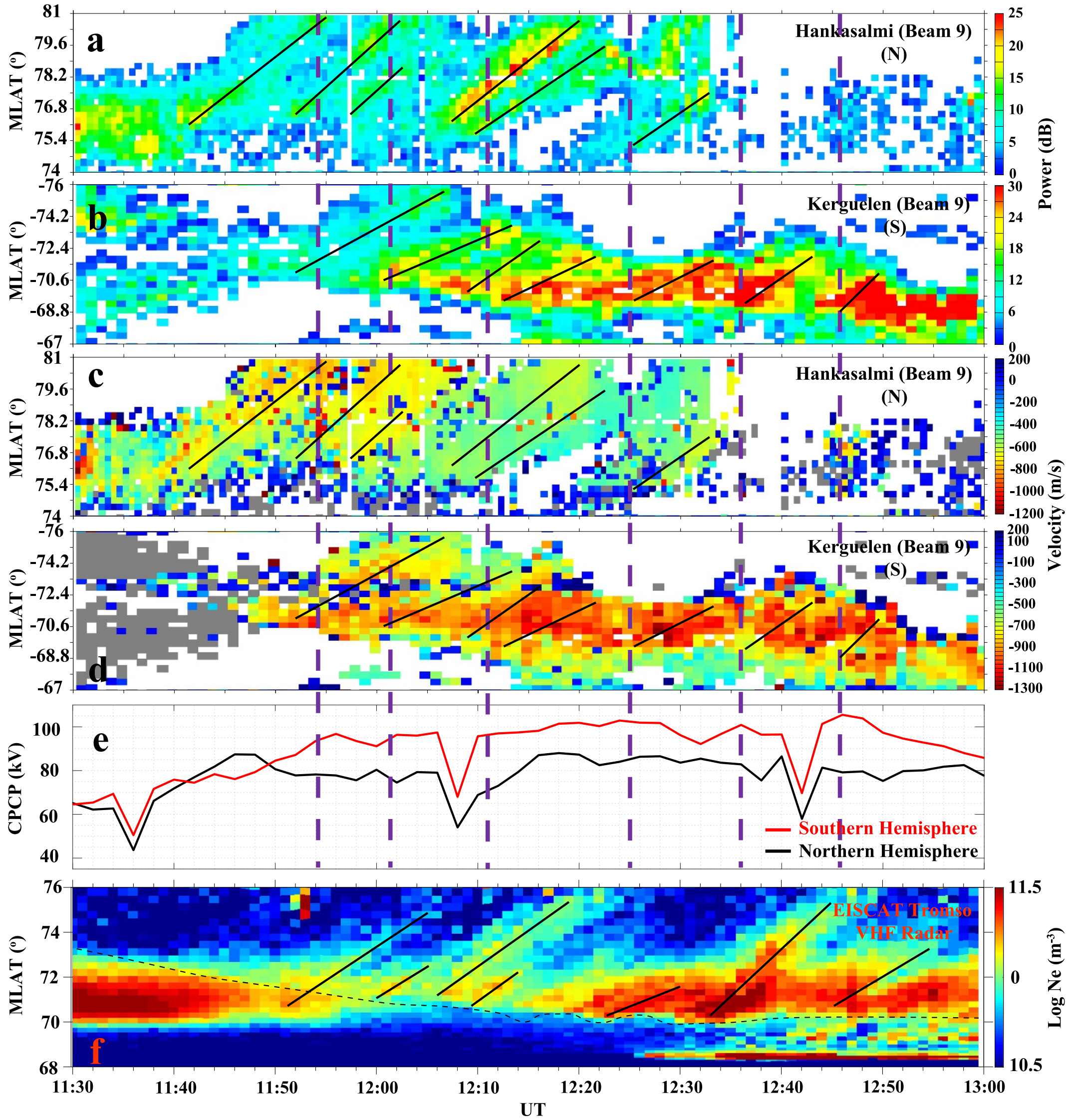

Figure 3. (a and b) Backscatter power and (c and d) line-of-sight (l-o-s) Doppler velocity observations of the HAN radar in the Northern Hemisphere and the KER Super Dual Auroral Radar Network (SuperDARN) radar in the Southern Hemisphere. The grey and white regions respectively represent SuperDARN ground backscatter and no data. The black solid lines highlight the Poleward Moving Radar Auroral Form (PMRAF) events. (e) Cross polar cap potential derived from the SuperDARN velocity measurements and obtained from the "map potential" algorithm. The purple dotted lines highlight the approximate time when each PMRAFs began to appear. (f) Line-of-sight ion velocity observed by the EISCAT Very-High Frequency radar.

Figure 3e shows the CPCP derived from the SuperDARN measurements and obtained from the "map potential" algorithm (Ruohoniemi & Baker, 1998). Before about 11:42 UT, the variation and magnitudes of CPCP in the Northern and Southern Hemispheres were almost the same. After the appearance of the PMRAFs, the CPCP in both hemispheres increased, and the CPCP in the Southern Hemisphere remained significantly higher than that in the Northern Hemisphere. Generally, the total open flux in both hemispheres should be the same. Such a difference in this event may be due to the fact that most of the SuperDARN echo signals in the Northern and Southern Hemispheres were concentrated on the dayside during this period, which cannot capture the complete flow velocity data, so the CPCP may have some differences with the actual value. It is certain that the flux was transferred into the polar cap faster in the Southern Hemisphere in a short period of time (~1 hr) near the cusp. Moreover, the PMRAFs in the Northern and Southern hemispheres seem to correspond, and the purple dotted lines highlight the approximate time when each PMRAFs began to appear, and almost all of them were consistent with the enhanced or the maintenance of CPCP. Note that these purple lines are defined mainly according to the observations in the Southern Hemisphere. Since more PMRAFs with higher Power were observed in the Southern Hemisphere, we marked them for comparison to see if there were the corresponding structures in the Northern Hemisphere. It should ideally be a one-to-one relationship between the PMRAFs and CPCP enhancement, but due to the resolution and limitations of the SuperDARN model, there is a possibility that multiple PMRAFs events corresponded to one CPCP enhancement. Note that at about 12:08 and 12:41 UT, the CPCP suddenly dropped. We checked the SuperDARN velocity data and did not find obvious anomalies. We speculate that this may be due to model limitations and the reduced data coverage elsewhere in the polar region. Moreover, during the observation of the PMRAFs, IMF By was not large (clock angle varied between 180° and 220°). Based on the IMF configuration and the previous studies (Crooker, 1979; Fear et al., 2012; Fuselier et al., 2021), we infer that the observed ionospheric characteristics are likely related to the magnetopause reconnection occurring near the magnetic equator in the two hemispheres, which is different from the work of Wild et al. (2003), where the clock angle was close to 100°.

To clearly demonstrate the polar ionospheric convection, Figure 4 shows a series of streamlines and vectors of the ionospheric flows during 11:30–13:00 UT for the Northern Hemisphere and Southern Hemisphere derived from SuperDARN. The time delay from the ACE satellite to the ionospheric response was approximately 70 min, which included the entire period from the propagation of solar wind and IMF data from the ACE satellite to the Earth's ionosphere, as well as the response time of the polar ionospheric convection. Noon is located at the top of each panel. In the Northern Hemisphere, around 11:40 UT, the l-o-s Doppler velocity began to enhance, reaching approximately 600 m/s. The velocity enhancement in the Southern Hemisphere was slightly later than that in the Northern Hemisphere, starting at about 11:50 UT, and the velocity enhancement exceeded 1,000 m/s. In the Southern Hemisphere, the westward flows (∼15 MLT) near the duskside sector intensified first, and then the anti-sunward flows near noon (∼12 MLT) intensified, while there is no similar feature in the Northern Hemisphere.

4. Discussion

In this event, the PMRAFs observed by the SuperDARN radars in the Northern and Southern Hemispheres seem to show a one-to-one correspondence. This can be explained by the axial orientation of the magnetopause flux ropes: when the IMF clock angle was near 180° (southward IMF), reconnection was favored near the dayside subsolar region, producing flux ropes whose axes are aligned roughly dusk-dawn and located near the equatorial plane (Guo et al., 2021). The energy and plasma are then "projected" at similar rates to the polar ionosphere of both hemispheres via Alfvén waves (Teh et al., 2023), resulting in PMRAFs sequences that are coincident in time (Zou et al., 2023). In this event, the IMF clock angle changed between 180° and 220°. Based on the IMF configuration and the previous studies (Crooker, 1979; Fear et al., 2012; Fuselier et al., 2021), reconnection theory predicts that there will be signatures in both hemispheres. The observed ionospheric characteristics in this event confirm these are the case for reconnection that can be inferred to be occurring based on the previous studies, and likely related to the magnetopause reconnection occurring near the magnetic equator in the two hemispheres, with the resulting flux ropes coupling energy into the polar ionosphere of both hemispheres. This observational result helps further understand how reconnection energy propagates toward polar regions within such clock angle ranges.

The PMPCEs observed by the VHF radar and the PMRAFs observed by the SuperDARN radar are ionospheric signatures of FTEs generated by magnetopause reconnection (Zhang et al., 2011; Zou et al., 2023). In this event, there were no obvious PMRAFs events observed by the Northern Hemisphere HAN SuperDARN radar after 12:35 UT, which is consistent with the radar field-of-view entering the afternoon sector around that time (MLT = UT + 3 hr). Because the negative IMF By moved the cusp (convection throat in the dayside connection pattern) to earlier MLT in the Northern Hemisphere, and later MLT in the Southern Hemisphere (Park et al., 2010; Watanabe et al., 2007). Thus, the PMRAFs first disappeared in the Northern Hemisphere at 12:35 UT and later disappeared in the Southern Hemisphere. It is interesting that the EISCAT VHF radar detected a sporadic E layer (Es) after ∼12:25 UT. The Es influences the SuperDARN HF backscatter signal, preventing the ability to detect the ionosphere at greater distances or higher heights (Kunduri et al., 2023).

SuperDARN data show that the occurrence of a series of FTEs seems to enhance the CPCP, and the contribution of these events has been calculated in previous studies (Lockwood et al., 1995; Newell and Sibeck, 1993). These results also show that the higher voltage and flow in the Southern Hemisphere (summer hemisphere) for a short

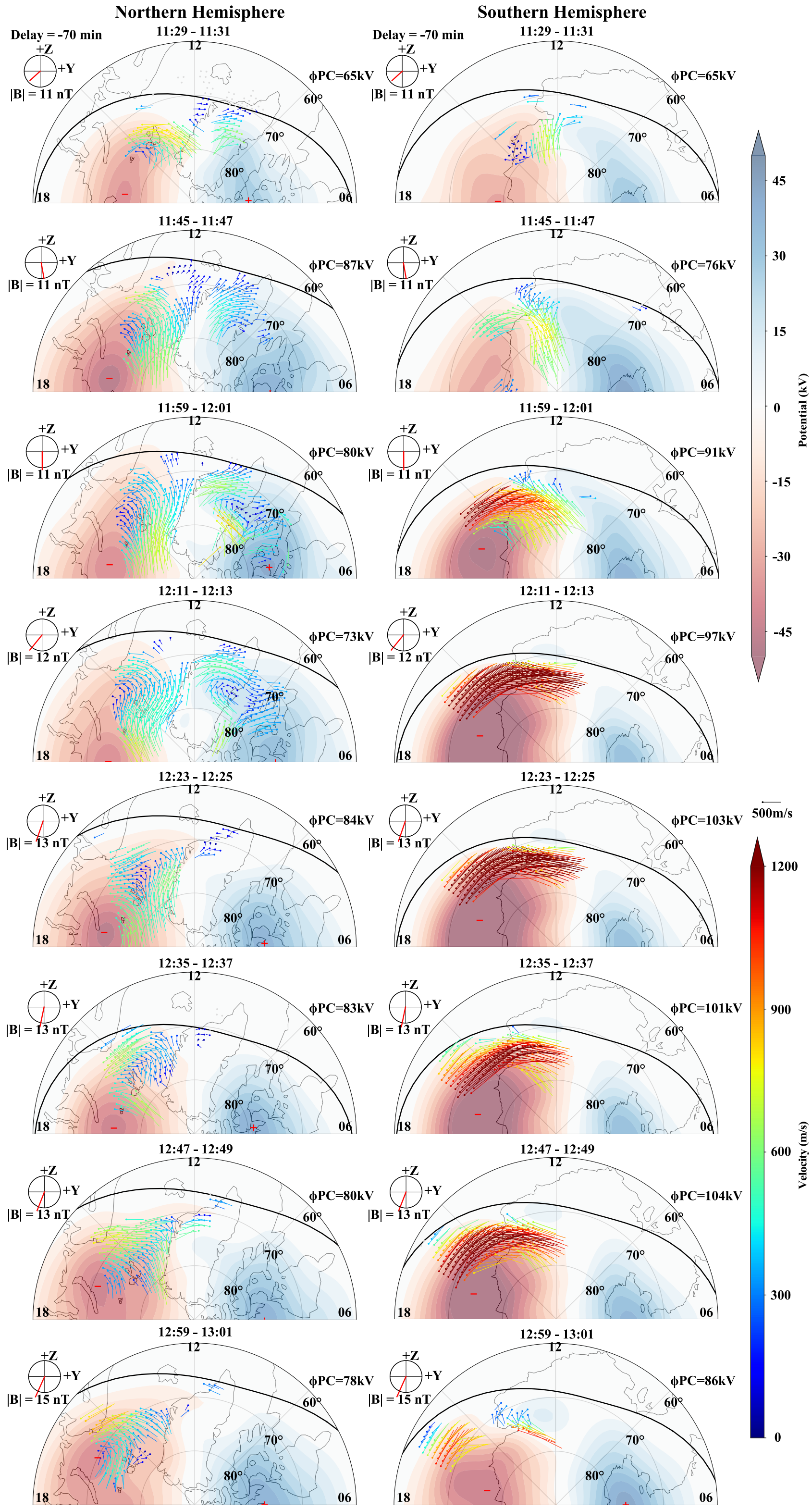

Figure 4. A series of streamlines and ionospheric flow vectors during 11:30-13:00 UT for the Northern Hemisphere (left) and Southern Hemisphere (right) derived from Super Dual Auroral Radar Network. The interplanetary magnetic field conditions and the cross polar cap potential are displayed respectively in the upper left and upper right corners of each panel. The black lines highlight the Heppner-Maynard Boundary.

time, which implies that the flux was transferred into the polar cap faster. Note that since there were fewer SuperDARN radar echo signals on the nightside, we can only determine the situation on the dayside, and the nightside was only roughly analyzed based on the SuperDARN model results. There are three points to consider: (a) Conductivity effect: the conductivity is higher in summer (Sheng et al., 2014), which increases Joule heating (Cosgrove et al., 2009), causing differences in the coupling efficiency between the two hemispheres. However, before the PMRAFs events were observed by SuperDARN, the CPCP of the two Hemispheres were basically equal, suggesting that the hemispheric asymmetry of conductivity was not the main factor; (b) Magnetic reconnection kink degree: in the winter hemisphere, the newly reconnected flux tubes have a larger "kink" and take a longer time to straighten out; (c) During the observation of the PMRAFs, both SuperDARN radar echoes were more in the duskside sector. Under the condition of IMF By < 0 (clock angle varied between 180° and 220°), the polar convection throat region in the Southern Hemisphere is closer to the duskside (Park et al., 2010; Watanabe et al., 2007), so it is possible that a stronger ionospheric flow response is more likely to be observed. Therefore, the CPCP given by the SuperDARN convection model may be larger. Moreover, this event occurred during the initial phase of a magnetic storm. During the initial phase of the magnetic storm, the CPCP will increase (Orr et al., 2023), but there is not sufficient work to indicate that it would cause a difference in the CPCP between the Northern and Southern hemispheres. These analyses of the factors that may cause the CPCP differences between the two hemispheres provide applicable observational evidence for improving the empirical model of the polar convection pattern. In the future, more statistical and simulation data need to be combined to quantitatively measure and quantify these hemispheric differences.

5. Conclusion

This work used EISCAT and SuperDARN radar observations to present observational evidence of conjugate ionospheric responses to the dayside magnetopause reconnection in both the Northern and Southern Hemispheres under southward IMF conditions with negative IMF By. The one-to-one correspondence between ionospheric signatures (PMRAFs and PMPCEs) of FTEs in the two hemispheres indicates that energy and plasma from reconnection are coupled to both polar ionospheres. Our results demonstrate that the occurrence of consecutive FTEs contributes to the convection and voltage in the polar regions, with the hemispheric asymmetry: the Southern Hemisphere (summer hemisphere) shows faster transport of reconnected magnetic flux tubes for a short time near the cusp. This asymmetry may be related to different factors such as the kink degree of newly reconnected flux tubes in the two hemispheres and the SuperDARN radar echoes coverage with the polar convection throat region.

Conflict of Interest

The authors declare no conflicts of interest relevant to this study.

Availability Statement

The IMF data are available at the NASA CDAWeb site via https://cdaweb.gsfc.nasa.gov/sp_phys/data/ace/ (NASA, 2026). The EISCAT VHF radar data are available at CEDAR Madrigal via http://cedar.openmadrigal.org/list/ (registering personal information and choosing "EISCAT Tromsø VHF IS radar") (Ingemar Häggström, 2004). The SuperDARN data is available at https://www.frdr-dfdr.ca/repo/collection/superdarn?order=DESC&sort=1 (choosing "SuperDARN 2004 DAT," then choosing "Download with Globus," and logging in) (Super Dual Auroral Radar Network, 2021).

Acknowledgments
The work in China was supported by the National Key R&D Program of China (Grant 2025YFF0510700), the National Natural Science Foundation of China (Grants 42120104003, 42325404, 42504166, 42474219, W2511046), the Chinese Meridian Project, the China Postdoctoral Science Foundation (Grant 2025M770391), the Basic Research Project (Grant DLCGZJYY-2024-038-02) and the Arctic Yellow River Earth System National Observation and Research Station (Grant YRNORS-20242606). The authors acknowledge the use of SuperDARN data. SuperDARN is a collection of radars funded by the national scientific funding agencies of Australia, Canada, China, France, Italy, Japan, Norway, South Africa, the United Kingdom and the United States of America.

References

Carlson, H. C., Oksavik, K., Moen, J., & Pedersen, T. (2004). Ionospheric patch formation: Direct measurements of the origin of a polar cap patch. *Geophysical Research Letters*, *31*(8), L08806. https://doi.org/10.1029/2003GL018166

Carlson, H. C., Oksavik, K., Moen, J., van Eyken, A. P., & Guio, P. (2002). ESR mapping of polar-cap patches in the dark cusp. *Geophysical Research Letters*, *29*(10), 1386. https://doi.org/10.1029/2001GL014087

Chisham, G., Lester, M., Milan, S. E., Freeman, M. P., Bristow, W. A., Grocott, A., et al. (2007). A decade of the super dual auroral radar network (SuperDARN): Scientific achievements, new techniques and future directions. *Surveys in Geophysics*, *28*(1), 33–109. https://doi.org/10.1007/s10712-007-9017-8

Cosgrove, R. B., Lu, G., Bahcivan, H., Matsuo, T., Heinselman, C. J., & McCready, M. A. (2009). Comparison of AMIE-modeled and Sondrestrom-measured Joule heating: A study in model resolution and electric field–conductivity correlation. *Journal of Geophysical Research*, *114*(A4), A04316. https://doi.org/10.1029/2008JA013508

Crooker, N. U. (1979). Dayside merging and cusp geometry. *Journal of Geophysical Research*, *84*(A3), 951–959. https://doi.org/10.1029/ja084ia03p00951

Davis, C. J., & Lockwood, M. (1996). Predicted signatures of pulsed reconnection in ESR data. *Annales Geophysicae*, *14*(12), 1246–1256. https://doi.org/10.1007/s00585-996-1246-5

Drury, E. E., Mende, S. B., Frey, H. U., & Doolittle, J. H. (2003). Southern hemisphere poleward moving auroral forms. *Journal of Geophysical Research*, *108*(A3), 1114. https://doi.org/10.1029/2001JA007536

Dungey, J. W. (1961). Interplanetary magnetic field and the auroral zones. *Physical Review Letters*, *6*(2), 47–48. https://doi.org/10.1103/physrevlett.6.47

Elphic, R. C., Lockwood, M., Cowley, S. W. H., & Sandholt, P. E. (1990). Flux transfer events at the magnetopause and in the ionosphere. *Geophysical Research Letters*, *17*(12), 2241–2244. https://doi.org/10.1029/GL017i012p02241

Fasel, G. J. (1995). Dayside poleward moving auroral forms: A statistical study. *Journal of Geophysical Research*, *100*(A7), 11891–11905. https://doi.org/10.1029/95JA00854

Fear, R. C., Palmroth, M., & Milan, S. E. (2012). Seasonal and clock angle control of the location of flux transfer event signatures at the magnetopause. *Journal of Geophysical Research*, *117*(A4), 7705. https://doi.org/10.1029/2011JA017235

Fear, R. C., Trenchi, L., Coxon, J. C., & Milan, S. E. (2017). How much flux does a flux transfer event transfer? *Journal of Geophysical Research*, *122*(12), 12310–12327. https://doi.org/10.1002/2017JA024730

Folkestad, K., Hagfors, T., & Westerlund, S. (1983). EISCAT: An updated description of technical characteristics and operational capabilities. *Radio Science*, *18*(6), 867–879. https://doi.org/10.1029/RS018i006p00867

Fuselier, S. A., Webster, J. M., Trattner, K. J., Petrinec, S. M., Genestreti, K. J., Pritchard, K. R., et al. (2021). Reconnection X-line orientations at the Earth's magnetopause. *Journal of Geophysical Research*, *126*(12), e2021JA029789. https://doi.org/10.1029/2021JA029789

Glassmeier, K.-H., & Stellmacher, M. (1996). Mapping flux transfer events to the ionosphere. *Advances in Space Research*, *18*(8), 151–160. https://doi.org/10.1016/0273-1177(95)00983-3

Greenwald, R. A., Baker, K. B., Dudeney, J. R., Pinnock, M., Jones, T. B., Thomas, E. C., et al. (1995). DARN/SuperDARN: A global view of the dynamics of high-latitude convection. *Space Science Reviews*, *71*(1–4), 761–796. https://doi.org/10.1007/BF00751350

Greenwald, R. A., Baker, K. B., Ruohoniemi, J. M., Dudeney, J. R., Pinnock, M., Mattin, N., et al. (1990). Simultaneous conjugate observations of dynamic variations in high-latitude dayside convection due to changes in IMF By. *Journal of Geophysical Research*, *95*(A6), 8057–8072. https://doi.org/10.1029/ja095ia06p08057

Guo, J., Lu, S., Lu, Q., Lin, Y., Wang, X., Huang, K., et al. (2021). Structure and coalescence of magnetopause flux ropes and their dependence on IMF clock angle: Three-dimensional global hybrid simulations. *Journal of Geophysical Research*, *126*(2), e2020JA028670. https://doi.org/10.1029/2020JA028670

Haerendel, G., Paschmann, G., Sckopke, N., Rosenbauer, H., & Hedgecock, P. (1978). The frontside boundary layer of the magnetosphere and the problem of reconnection. *Journal of Geophysical Research*, *83*(A7), 3195–3216. https://doi.org/10.1029/JA083iA07p03195

Ingemar Häggström (2004). EISCAT scientific association. *Data From the CEDAR Madrigal Database*.

Komar, C. M., & Cassak, P. A. (2016). The local dayside reconnection rate for oblique interplanetary magnetic fields. *Journal of Geophysical Research*, *121*(6), 5105–5120. https://doi.org/10.1002/2016JA022530

Kunduri, B. S. R., Erickson, P. J., Baker, J. B., Ruohoniemi, J. M., Galkin, I., & Sterne, K. (2023). Dynamics of mid-latitude Sporadic-E and its impact on HF propagation in the North American sector. *Journal of Geophysical Research*, *128*(9), e2023JA031455. https://doi.org/10.1029/2023ja031455

Liou, K., Newell, P. T., Meng, C.-I., Brittnacher, M., & Parks, G. (1998). Characteristics of the solar wind controlled auroral emissions. *Journal of Geophysical Research*, *103*(A8), 17543–17557. https://doi.org/10.1029/98JA01388

Liu, Y. H., Hesse, M., Genestreti, K., Nakamura, R., Burch, J. L., Cassak, P. A., et al. (2025). Ohm's law, the reconnection rate, and energy conversion in collisionless magnetic reconnection. *Space Science Reviews*, *221*(1), 16. https://doi.org/10.1007/s11214-025-01142-0

Lockwood, M., Cowley, S. W. H., Smith, M. F., Rijnbeek, R. P., & Elphic, R. C. (1995). The contribution of flux transfer events to convection. *Geophysical Research Letters*, *22*(10), 1185–1188. https://doi.org/10.1029/95GL01008

Lockwood, M., McCrea, I. W., Milan, S. E., Moen, J., Cerisier, J. C., & Thorolfsson, A. (2000). Plasma structure within poleward-moving cusp-cleft auroral transients: EISCAT Svalbard radar observations and an explanation in terms of large local time extent of events. *Annales Geophysicae*, *18*(9), 1027–1042. https://doi.org/10.1007/s00585-000-1027-5

Lockwood, M., Sandholt, P. E., Cowley, S. W. H., & Oguti, T. (1989). Interplanetary magnetic field control of dayside auroral activity and the transfer of momentum across the dayside aurora magnetopause. *Planetary and Space Science*, *37*(11), 1347–1364. https://doi.org/10.1016/0032-0633(89)90106-2

Lyon, J. G. (2000). The solar wind-magnetosphere-ionosphere system. *Science*, *288*(5473), 1987–1991. https://doi.org/10.1126/science.288.5473.1987

Mende, S. B., Frey, H. U., & Angelopoulos, V. (2016). Source of the dayside cusp aurora. *Journal of Geophysical Research*, *121*(8), 7728–7738. https://doi.org/10.1002/2016JA022657

Milan, S. E., Gosling, J. S., & Hubert, B. (2012). Relationship between interplanetary parameters and the magnetopause reconnection rate quantified from observations of the expanding polar cap. *Journal of Geophysical Research*, *117*(A3), A03226. https://doi.org/10.1029/2011JA017082

Milan, S. E., Lester, M., Cowley, S. W. H., & Brittnacher, M. (2000). Convection and auroral response to a southward turning of the IMF: Polar UVI, CUTLASS and IMAGE signatures of transient flux transfer at the magnetopause. *Journal of Geophysical Research*, *105*(A7), 15741–15756. https://doi.org/10.1029/2000JA900022

Milan, S. E., Yeoman, T. K., Lester, M., Thomas, E. C., & Jones, T. B. (1997). Initial backscatter occurrence statistics from the CUTLASS HF radars. *Annales Geophysicae*, *15*(6), 703–718. https://doi.org/10.1007/s00585-997-0703-0

Moen, J., Lockwood, M., Oksavik, K., Carlson, H. C., Denig, W. F., van Eyken, A. P., & McCrea, I. W. (2004). The dynamics and relationships of precipitation, temperature and convection boundaries in the dayside auroral ionosphere. *Annales Geophysicae*, *22*(6), 1973–1987. https://doi.org/10.5194/angeo-22-1973-2004

Moen, J., Oksavik, K., & Carlson, H. C. (2004). On the relationship between ion upflow events and cusp auroral transients. *Geophysical Research Letters*, *31*(11), L11808. https://doi.org/10.1029/2004GL020129

Moen, J., Rinne, Y., Carlson, H. C., Oksavik, K., Fujii, R., & Opgenoorth, H. (2008). On the relationship between thin Birkeland current arcs and reversed flow channels in the winter cusp/cleft ionosphere. *Journal of Geophysical Research*, *113*(A9), A09220. https://doi.org/10.1029/2008JA013061

Mozer, F. S., & Pritchett, P. L. (2010). Magnetic field reconnection: A first-principles perspective. *Physics Today*, *63*(6), 34–39. https://doi.org/10.1063/1.3455250

NASA. (2026). Solar wind and IMF data from the NASA CDAWeb site [Dataset]. Retrieved from https://cdaweb.gsfc.nasa.gov/sp_phys/data/ace/

Newell, P. T., & Sibeck, D. G. (1993). Upper limits on the contribution of flux transfer events to ionospheric convection. *Geophysical Research Letters*, *20*(23), 2829–2832. https://doi.org/10.1029/93GL02843

Oksavik, K., Moen, J., & Carlson, H. C. (2004). High-resolution observations of the small-scale flow pattern associated with a poleward moving auroral form in the cusp. *Geophysical Research Letters*, *31*(11), L11807. https://doi.org/10.1029/2004GL019838

Oksavik, K., Moen, J., Carlson, H. C., Greenwald, R. A., Milan, S. E., Lester, M., et al. (2005). Multi-instrument mapping of the small-scale flow dynamics related to a cusp auroral transient. *Annales Geophysicae*, *23*(7), 2657–2670. https://doi.org/10.5194/angeo-23-2657-2005

Oksavik, K., Moen, J. I., Rekaa, E. H., Carlson, H. C., & Lester, M. (2011). Reversed flow events in the cusp ionosphere detected by SuperDARN HF radars. *Journal of Geophysical Research*, *116*(A12), A12303. https://doi.org/10.1029/2011JA016788

Orr, L., Grocott, A., Walach, M.-T., Chisham, G., Freeman, M. P., Lam, M. M., & Shore, R. M. (2023). A quantitative comparison of high latitude electric field models during a large geomagnetic storm. *Space Weather*, *21*(1), e2022SW003301. https://doi.org/10.1029/2022SW003301

Park, K. S., Ogino, T., & Kim, Y. H. (2010). Effects of the dipole tilt and northward and duskward IMF on dayside magnetic reconnection in a global MHD simulation. *Journal of Geophysical Research*, *115*(A2), A02208. https://doi.org/10.1029/2009JA014212

Pinnock, M., Rodger, A. S., Dudeney, J. R., Rich, F., & Baker, K. B. (1995). High spatial and temporal resolution observations of the ionospheric cusp. *Annales Geophysicae*, *13*(9), 919–925. https://doi.org/10.1007/s005850050231

Provan, G., Yeoman, T. K., & Milan, S. E. (1998). CUTLASS Finland radar observations of the ionospheric signatures of flux transfer events and the resulting plasma flows. *Annales Geophysicae*, *16*(11), 1411–1422. https://doi.org/10.1007/s00585-998-1411-0

Rishbeth, H., & Van Eyken, A. P. (1993). EISCAT: Early history and the first ten years of operation. *Journal of Atmospheric and Terrestrial Physics*, *55*(4–5), 525–542. https://doi.org/10.1016/0021-9169(93)90002-G

Ruohoniemi, J. M., & Baker, K. B. (1998). Large-scale imaging of high-latitude convection with super dual auroral radar network HF radar observations. *Journal of Geophysical Research*, *103*(A9), 20797–20811. https://doi.org/10.1029/98JA01288

Russell, C. T., & Elphic, R. C. (1978). Initial ISEE magnetometer results: Magnetopause observations. *Space Science Reviews*, *22*, 681–715.

Sandholt, P. E., & Farrugia, C. J. (2007). Poleward moving auroral forms (PMAFs) revisited: Responses of aurorae, plasma convection and Birkeland currents in the pre- and postnoon sectors under positive and negative IMF By conditions. *Annales Geophysicae*, *25*(7), 1629–1652. https://doi.org/10.5194/angeo-25-1629-2007

Sheng, C., Deng, Y., Yue, X. A., & Huang, Y. S. (2014). Height-integrated Pedersen conductivity in both E and F regions from COSMIC observations. *Journal of Atmospheric and Solar-Terrestrial Physics*, *115–116*, 79–86. https://doi.org/10.1016/j.jastp.2013.12.013

Super Dual Auroral Radar Network. (2021). SuperDARN 2004 DAT [Dataset]. *Federated Research Data Repository*. https://doi.org/10.20383/102.0460

Teh, W.-L., Zhang, W., & Fu, H. (2023). Kinetic and shear alfvén waves in a large guide-field reconnection at earth's magnetopause. *Astrophysical Journal*, *959*(2), 68. https://doi.org/10.3847/1538-4357/ad09b4

Watanabe, M., Sofko, G. J., Kabin, K., Rankin, R., Ridley, A. J., Clauer, C. R., et al. (2007). Origin of the interhemispheric potential mismatch of merging cells for interplanetary magnetic field BY -dominated periods. *Journal of Geophysical Research*, *112*(A10), A10205. https://doi.org/10.1029/2006JA012179

Wild, J. A., Milan, S. E., Cowley, S. W. H., Dunlop, M. W., Owen, C. J., Bosqued, J. M., et al. (2003). Coordinated interhemispheric SuperDARN radar observations of the ionospheric response to flux transfer events observed by the cluster spacecraft at the high-latitude magnetopause. *Annales Geophysicae*, *21*(8), 1807–1826. https://doi.org/10.5194/angeo-21-1807-2003

Yamada, M., Kulsrud, R., & Ji, H. (2010). Magnetic reconnection. *Reviews of Modern Physics*, *82*(1), 603–664. https://doi.org/10.1103/RevModPhys.82.603

Zhang, Q.-H., Zhang, B.-C., Liu, R.-Y., Dunlop, M. W., Lockwood, M., Moen, J., et al. (2011). On the importance of IMF |BY| in polar cap patch formation. *Journal of Geophysical Research*, *116*(A5), A05308. https://doi.org/10.1029/2010JA016287

Zhang, Q.-H., Zhang, B.-C., Lockwood, M., Hu, H.-Q., Moen, J. I., Ruohoniemi, J. M., et al. (2013). Direct observations of the evolution of polar cap ionization patches. *Science*, *339*(6127), 1597–1600. https://doi.org/10.1126/science.1231487

Zou, Y., Chen, L.-J., Walsh, B. M., Burkholder, B., Ma, Y.-Z., Bristow, W. A., et al. (2023). Hemispheric symmetry and asymmetry of poleward moving radar auroral forms (PMRAFs) and associated polar cap patches during a geomagnetic storm. *Frontiers in Physics*, *11*, 1174209. https://doi.org/10.3389/fphy.2023.1174209